DFT PREPROCESSING FOR HIGH-RESOLUTION FREQUENCY ESTIMATION

Arnab K. Shaw and *Wei Xia*

Department of Electrical Engineering, Wright State University, Dayton, OH 45435.
Phone : (513) 873-5064, e-mail : ashaw@valhalla.cs.wright.edu

ABSTRACT

This work considers the use of the DFT of the Autocorrelation (AC) matrix (DFT-of-AC) for extracting the signal and noise subspaces. It is shown that when DFT preprocessed data is incorporated within the frameworks of Minimum-Norm (MNM) or Prony's methods, improved high-resolution estimates are obtained. Furthermore, if the signal-subspace part of the DFT-of-AC vectors are used in place of eigenvectors in MNM, the high-resolution performance is further enhanced. Theoretical Perturbation Analysis of the DFT-based MNM (D-MNM) shows that the estimates are unbiased and, furthermore the theoretical Mean-Squared Error results indicate improved high-resolution performance, especially at low SNR.

I. Introduction

The primary objective of this work is to study whether DFT preprocessed data can be effectively incorporated within the algorithmic framework of high resolution frequency and Angles-of-Arrival (AOA) estimation methods. Some well-known existing approaches, such as the Minimum-Norm method (E-MNM) or MUSIC, extract the signal and noise subspace information from the eigenvectors of the Autocorrelation (AC) matrices. However, recent studies have shown that the DFT of the AC-matrix (DFT-of-AC) essentially performs an equivalent task of extracting and decoupling the signal and noise subspace information [6, 7] (also see [8] and [10]). When the DFT-of-AC vectors with larger norms were used in place of the eigenvectors in the Minimum-Norm framework, almost equivalent or better high-resolution AOA estimates were produced [6, 7]. This paper demonstrates that the performance of the original E-MNM may also be improved upon if DFT-preprocessed AC-matrix is used. Similar improvement in performance is also exhibited by the Prony's method when DFT-preprocessed data is incorporated.

In the final part of this paper, we outline the main results of theoretical Perturbation Analysis of the estimates produced by the D-MNM algorithm. Firstly, the bias and the mean-squared-error (MSE) in the estimates of the AOAs are analyzed. Then the error in the roots of the polynomial formed in the intermediate step of D-MNM is examined. The results obtained so far indicate that the high-resolution performance of D-MNM is uniformly superior than its eigen-based counterpart, especially at low SNR. The performance is also superior than the eigen-based root-MUSIC method at low SNR. The theoretical analysis closely matches the performance with simulated data.

The major significance of the D-MNM algorithm is that, no complicated iterative optimization is needed and the signal-subspace information is extracted only by a ***single matrix multiplication.*** Hence, hardware implementation of D-MNM for real-time high-resolution AOA/Frequency estimation may be feasible with currently available technology.

This research was partly supported by AFOSR-F49620-90-C-09076 and by AFOSR-F49620-93-1-0014.

II. Problem Definition

Let the signals sampled at m^{th} instant of time at N equally spaced sensors form a 'snapshot' vector defined as,

$$\mathbf{x}_m \triangleq [x_m(0)\ x_m(1)\ \ldots\ x_m(N-1)]^T, \quad \text{where} \tag{1}$$

$$x_m(n) = \tilde{x}_m(n) + z_m(n), \tag{2}$$

$z_m(n)$ represents noise and for p narrowband sources the signal can be expressed as [1],

$$\tilde{x}_m(n) = \sum_{i=1}^{p} a_m(i) e^{j\frac{2\pi d}{\lambda}(n-\frac{N+1}{2})\sin\theta_i + j\phi_m(i)}, \tag{3}$$

$$= \sum_{i=1}^{p} A_{im} e^{j\omega_i n},\ n = 0, 1, .., N-1 \tag{4}$$

where, d and λ denote the spacing between sensor elements and the wavelength of radiation of the received signals, respectively. θ_i, $a_m(i)$ and $\phi_m(i)$ denote the AOAs, amplitude and the random phase angle, respectively, of the i^{th} source, $\omega_i \triangleq \frac{2\pi d}{\lambda}\sin\theta_i$ and $A_{im} \triangleq A_m(i)e^{-j\frac{2\pi d}{\lambda}\left(\frac{N+1}{2}\right)\sin\theta_i + j\phi_m(i)}$. The noise $z_m(n)$ is assumed to be zero-mean and uncorrelated with the source signals. In matrix form, the observations can be modeled as,

$$\tilde{\mathbf{X}} \triangleq \mathbf{TA} \quad \text{where,} \quad \mathbf{A} \triangleq [\mathbf{a}_1\ \mathbf{a}_2\ \ldots\ \mathbf{a}_M] \tag{5}$$

$$\mathbf{T} \triangleq \begin{bmatrix} 1 & \ldots & 1 \\ e^{j\omega_1} & \ldots & e^{j\omega_p} \\ \vdots & \ddots & \vdots \\ e^{j\omega_1(N-1)} & \ldots & e^{j\omega_p(N-1)} \end{bmatrix} \triangleq [\mathbf{t}_1\ \mathbf{t}_2\ \cdots\ \mathbf{t}_p], \tag{6}$$

$\mathbf{a}_m \triangleq [A_{1m}\ A_{2m}\ldots\ A_{pm}]^T$ for, $m = 1, 2, \ldots, M$. Note that, $\omega_i = \pi\ \sin\theta_i$ if, $d = \frac{\lambda}{2}$. The spatial covariance matrix can be estimated as,

1058-6393/95 $4.00 © 1995 IEEE

$$\mathbf{C} \triangleq \frac{1}{M}(\mathbf{X}\mathbf{X}^H) \triangleq \frac{1}{M}\sum_{m=1}^{M}\mathbf{x}_m\mathbf{x}_m^H. \quad (7)$$

Given the noisy observation matrix $\mathbf{X}$, the problem under consideration is to estimate the ω_i's and A_{im}'s. Existing eigen-based methods make use of the underlying properties of the $\mathbf{C}$ matrix. For the noiseless case, $\mathbf{C}$ is rank p and its eigen-decomposition can be written as,

$$\mathbf{CV} = [\lambda_1\mathbf{v}_1 \quad \cdots \quad \lambda_p\mathbf{v}_p \quad 0 \quad \cdots \quad 0] = \mathbf{\Lambda V}, \quad (8)$$

where, the λ_i's and $\mathbf{v}_i$'s denote the eigenvalues and eigenvectors, respectively. However, for noisy observations,

$$\mathbf{CV} = [\hat{\lambda}_1\mathbf{v}_1 \quad \cdots \quad \hat{\lambda}_p\mathbf{v}_p \quad \hat{\lambda}_{p+1}\mathbf{v}_{p+1} \quad \cdots \quad \hat{\lambda}_N\mathbf{v}_N] \quad (9)$$

where, the estimated eigenvalues are ordered as, $\hat{\lambda}_1 \geq \hat{\lambda}_2 \geq \cdots \hat{\lambda}_N$. The eigenvectors corresponding to the p largest eigenvalues are called the 'signal eigenvectors'. The other $(N-p)$ eigenvectors are known as the 'noise eigenvectors'.

III. The DFT-Based Minimum-Norm Method (D-MNM) [6, 7]

As a significant departure from existing eigen-based approaches, in this method the signal-subspace information is extracted from the DFT-of-AC matrix. The primary advantage is that this can be accomplished with a single matrix multiplication which eliminates the need for any computationally intensive calculation of eigenvectors.

III.1. Signal/Noise Subspaces from DFT-of-AC

Let the DFT matrix be denoted as,

$$\mathbf{D} \triangleq [\mathbf{e}_1 \quad \mathbf{e}_2 \quad \cdots \quad \mathbf{e}_N], \quad (10)$$

where, the elements of the k-th DFT-vector $\mathbf{e}_k$ is defined as, $\mathbf{e}_k(l) = e^{j\frac{2\pi}{N}kl}$, for $k,l = 0,1,2,\ldots,N-1$. It has been shown in [6, 7] that for the ideal case when the frequencies ω_is are all on the DFT bins and if there is no observation noise then, for large number of snapshots M, the DFT-of-AC has the following decomposition,

$$\mathbf{F} \triangleq \mathbf{CD} \triangleq [\mathbf{f}_1 \quad \mathbf{f}_2 \quad \cdots \quad \mathbf{f}_N] \quad (11)$$

$$\rightarrow [\Lambda_1\mathbf{u}_1 \quad \cdots \quad \Lambda_p\mathbf{u}_p \quad 0 \quad \cdots \quad 0] \quad (12)$$

where, the Λ_is and $\mathbf{u}_i$s are the lengths and unit vectors, respectively, of each $\mathbf{f}_i$. Note that the unit vectors in the matrix in (11) have been rearranged so that the zero/nonzero components are clustered together. Interestingly, this decomposition appears to be very similar to the usual Eigendecomposition of noiseless and ideal $\mathbf{C}$, as given by (8).

In general, the observations are noisy and the angular frequencies ω_is are arbitrarily spaced and hence, the decomposition in (11) or (12) will not hold. But the DFT-components ($\mathbf{f}_k$s) closer to the signal frequencies will tend to have larger norms and then the signal/noise subspace decomposition can be formed as :

$$\mathbf{F} \rightarrow [\Lambda_1\mathbf{u}_1 \quad \cdots \quad \Lambda_p\mathbf{u}_p \quad \Lambda_{p+1}\mathbf{u}_{p+1} \quad \cdots \quad \Lambda_N\mathbf{u}_N] \quad (13)$$

$$\triangleq \mathbf{\Lambda}[\mathbf{U}_S \mid \mathbf{U}_N] \quad (14)$$

where, $\Lambda_1 \geq \Lambda_2 \geq \cdots \geq \Lambda_N$ are the norms of the $\mathbf{f}_i$ vectors, $\mathbf{\Lambda}$ is a diagonal matrix with Λ_i's in the diagonal and $\mathbf{U}_S$ and $\mathbf{U}_N$ contain the signal and noise subspace vectors, respectively. It may be observed again that the decomposition in (13)-(14) is analogous to the eigen-based counterpart in (9).

III.2. DFT-Based Signal Subspaces in MNM Framework

The principal idea behind the original Minimum-Norm method [2, 4] is to form an appropriate 'noise-subspace' vector $\mathbf{d}$ which is orthogonal to the 'signal-subspace' defined by $\mathbf{U}_S$. Let, $D(z) \triangleq \sum_{k=1}^{N} d_k z^{-(k-1)}$ be an $(N-1)$-th order z-polynomial with p zeros at, $z_k = e^{j\omega_k}$, for, $k = 1, \ldots, p$, corresponding to the AOAs. The coefficient vector is denoted as,

$$\mathbf{d} \triangleq [d_1 \quad d_2 \quad \cdots \quad d_N]^T \quad (15)$$

where, $d_1 = 1$. The Minimum-Norm Method utilizes a orthogonal relationship between $\mathbf{d}$ and the signal-subspace formed by $\mathbf{U}_S$,

$$\mathbf{U}_S^H\mathbf{d} = \mathbf{0}. \quad (16)$$

This underdetermined set of equations has infinite number of solutions. According to [2], the following 'minimum-norm' solution that also minimizes the norm $\|\mathbf{d}\|^2$, possesses a desirable property that all its roots fall inside the unit circle :

$$\mathbf{d} = \begin{bmatrix} 1 \\ - - - - - - - - \\ -\ \mathbf{G}^H(\mathbf{G}\mathbf{G}^H)^{-1}\mathbf{g} \end{bmatrix}, \quad (17)$$

where, $\mathbf{U}_S^H$ is partitioned as, $\mathbf{U}_S^H \triangleq [\mathbf{g} \mid \mathbf{G}]$. Once $\mathbf{d}$ is estimated, the p roots of $D(z)$ closest to the unit circle are used to find the AOAs. It may be recalled that in E-MNM the signal-subspace eigenvectors $\mathbf{v}_1, \mathbf{v}_2, \ldots, \mathbf{v}_p$, as defined in (9) are used to form $\mathbf{U}_S$ [2, 4]. But in case of the proposed approach, no eigendecomposition is necessary. Post-multiplication of $\mathbf{C}$ by the DFT-matrix $\mathbf{D}$ is all that is required to extract the signal subspace in (13). Theoretical perturbation analysis of the D-MNM algorithm has been performed and the results are summarized in the Appendix.

III.3. Summary of the D-MNM Algorithm

- Form the Covariance Matrix estimate using forward-backward method [2, 9] :

$$\hat{\mathbf{C}} \triangleq \frac{1}{2M}\sum_{m=1}^{M}\mathbf{x}_m\mathbf{x}_m^H + \mathbf{x}_m^b\mathbf{x}_m^{b\,H}. \quad (18)$$

  The 'backward' vector is defined as $\mathbf{x}_m^b \triangleq \mathbf{J}\mathbf{x}_m^*$, where, $\mathbf{J}$ denotes the permutation matrix with 1's at the cross-diagonal entries and * denotes the complex-conjugate operation.

- Post-multiply $\mathbf{C}$ by the DFT matrix $\mathbf{D}$ to form the DFT-OF-AC matrix, $\mathbf{F} \triangleq \mathbf{CD}$.
- Form $\mathbf{U}_S$ as in (14) using the p unit vectors corresponding to the largest norms.
- Estimate the $\mathbf{d}$ vector using (17) and form the $D(z)$ polynomial using the elements of $\mathbf{d}$.

- Find the roots of $D(z)$. Pick the p roots closest to the unit circle to find the desired frequencies/AOAs.

IV. DFT Preprocessed MNM (P-MNM)

In this section we study if DFT preprocessing can be incorporated in the original eigen-based MNM to improve its performance. Let, $\mathbf{F}$ defined in (11) be partitioned as,

$$\mathbf{F} \triangleq [\mathbf{F}_S \mid \mathbf{F}_N] \tag{19}$$

where, $\mathbf{F}_S$ is formed with the $N_S(\geq p)$ largest-norm vectors of $\mathbf{F}$. Clearly, the signal component in the column space of $\mathbf{F}_S$ is 'enhanced' when compared with the entire $\mathbf{C}$ commonly used by E-MNM. However, $\mathbf{F}_S$ is rectangular and hence, the p largest left-eigenvectors of the SVD of $\mathbf{F}_S$ has to be used (in place of the eigenvectors of $\mathbf{C}$) to find the minimum-norm vector $\mathbf{d}$. Simulation results presented in Section VI indicate that for $N_S = \frac{N}{2}$, the performance of P-MNM is superior than that of the original E-MNM. But the best performance is obtained for $N_S = p$ when the performance coincides exactly with that of D-MNM which does not need any eigendecomposition but uses $\mathbf{F}_S$ directly.

IV.1. Summary of the P-MNM Algorithm

- Form the Covariance Matrix estimate using (18).
- Form the DFT-OF-AC matrix, $\mathbf{F} \triangleq \mathbf{CD}$.
- Form $\mathbf{W}_S$ using the N_S ($\geq p$) vectors of $\mathbf{F}$ having the largest norms.
- Perform SVD of $\mathbf{W}_S$ and form $\mathbf{U}_S$ using the p largest left-eigenvectors of $\mathbf{W}_S$.
- Estimate the $\mathbf{d}$ vector using (17) and form the $D(z)$ polynomial using the elements of $\mathbf{d}$.
- Find the roots of $D(z)$. Pick the p roots closest to the unit circle to find the desired frequencies/AOAs.

V. DFT Preprocessed Prony's Method (P-Prony)

Prony's method is perhaps the simplest of all high-resolution methods that rely of rooting of polynomials. Unlike MNM or Root-MUSIC, Prony's method requires rooting of only a p-th order z-polynomial. However, the performance of this method is known to degrade if the observation is noisy. But the discussion in the previous section suggests that considerable signal enhancement can be attained if $\mathbf{F}_S$ is formed with the p largest-norm vectors of $\mathbf{F}$. Hence, the columns of $\mathbf{F}_S$ can be used directly in Prony's method to obtain improved estimates of frequencies. The results included in the next section do confirm this hypothesis.

IV.1. Summary of the P-Prony Algorithm

- Form the Covariance Matrix estimate using (18).
- Form the DFT-OF-AC matrix, $\mathbf{F} \triangleq \mathbf{CD}$.
- Pick p vectors of $\mathbf{F}$ having to the largest norms.
- Apply standard Prony's by treating the p pre-processed DFT-of-AC vectors as 'data'.

VI. Simulation Results

VI.1. Simulation 1 : *Frequency and AOA Estimation*

Planewaves from $p = 2$ sources with $\theta_1 = 18°$ and $\theta_2 = 22°$ incident on N=8 sensors were modeled as in [2]. The number of snapshots, M=10. Fig. 1 compares E-MNM and D-MNM in terms of RMS values for 200 independent trials at different SNR values. The results indicate that the performance of D-MNM which does not require any Eigendecomposition, is somewhat better than that of E-MNM in this case. In fact, D-MNM was found to be more robust (in terms of bias, rms value and number of successful trials) at low SNR ranges. Figures 2 and 3 compare the results for E-MNM and P-MNM using $N_S = 4p$ and $N_S = p$, respectively. Clearly, the preprocessing step improves performance at low SNR. The best performance for P-MNM was observed at $N_S = p$ but interestingly, the results in case were found to be identical to that of D-MNM.

VI.2. Simulation 2 : *Frequency Estimation*

The performance of D-MNM is compared with the TK method [9] and CR bound using the data set,

$$y(n) = a_1 e^{j2\pi(0.5)n + j\frac{\pi}{4}} + a_2 e^{j2\pi(0.52)n} + w(n), \tag{20}$$

for, $n = 0, 1, \ldots, M-1$, where, $w(n)$ is complex white Gaussian noise with variance σ_w^2. The number of data samples used is, M=25 and five hundred independent noise realizations were used. Fig. 4 compares the RMSE values in dB. The results indicate threshold enhancement by D-MNM.

VI.3. Simulation 3 : *Comparison of Prony's and DFT Preprocessed Prony's Method*

In this case, the performance of the P-Prony algorithm is compared with the standard Prony's method via simulations using the same data set as in Simulation 2. The RMSE results for P-Prony and Prony's method are shown in Fig. 5 along with the CR bounds for the frequency at $f_1 = 0.52Hz$. Clearly, the P-Prony extends the performance threshold closer to the CR bound.

VI.4. Simulation 4 : *Perturbation Analysis with Small Number of Sensors*

The problem scenario is identical to as described in Simulation 1 for AOA estimation. For this case, $N = 8, M = 100$, and the AOAs are 18° and 22°. In these simulations the theoretical formulas for mean-squared error, as given in the Appendix are compared with the performance using simulated data. The results for various signal-to-noise ratios (SNR) are shown in Fig. 6. for the AOA at 18° for 200 independent trials. Note that data set considered in Simulation 4 had also been used in [3] for perturbation analysis of the eigen-based MNM and MUSIC. Fig. 6 indicates that for this example, the D-MNM method appears to have smaller squared error than E-MNM, especially at low SNR. In fact, the success rate was also higher for D-MNM when compared with E-MNM. Finally, it may be emphasized here that the theoretical predictions based on formulas given in the Appendix were found to be quite close to those obtained by computer simulations.

References

[1] S. Haykin et al, Editors, *Array Signal Processing*, Prentice-Hall, 1985.

[2] R. Kumaresan and D. W. Tufts, "Estimating the Angles of Arrival of Multiple Planewaves," *IEEE Transactions on Aerospace and Electronic Systems*, vol. AES-19, no .1, pp. 134-139, Jan., 1983.

[3] B. D. Rao, "Statistical Performance Analysis of the Minimum-Norm Method," *IEE Proceedings, Part-F*, vol. 136, Pt. F, no. 3, pp. 125-134, June 1989.

[4] S. S. Reddi, "Multiple Source Location- A Digital Approach," *IEEE Transactions on Aerospace and Electronic Systems*, vol. AES-15, no.1, pp. 95-105, 1979.

[5] R. O. Schmidt, "Multiple Emitter Location and Signal Parameter Estimation," *Proceedings of RADC Spectral Estimation Workshop*, pp. 243-258, Rome, New York, 1979.

[6] A. K. Shaw and W. Xia, "High-Resolution Angles of Arrival Estimation using Minimum-Norm Method Without Eigendecomposition," *IEEE International Conference on Acoustics, Speech and Signal Processing*, Adelaide, Australia, April, 1994.

[7] A. K. Shaw and W. Xia, "Minimum-Norm Method Without Eigendecomposition," *IEEE Signal Processing Letters*, vol. 1, no. 1, pp. 12-14, Jan. 1994.

[8] J. T. Karhunen and J. Joutsensalo, "Sinusoidal Frequency Estimation by Signal Subspace Approximation," *IEEE Transactions on Signal Processing*, vol. ASSP-35, no. 2, Feb..

[9] D. W. Tufts and R. Kumaresan, "Frequency Estimation of Multiple Sinusoids : Making Linear Prediction Perform Like Maximum Likelihood," *Proceedings of the IEEE*, vol. 70, pp. 975-989. Sept., 1982.

[10] D. W. Tufts and C. D. Melissinos, "Simple, Effective Computation of Principal Eigenvectors and their Eigenvalues and Application to High-Resolution Estimation of Frequencies," *IEEE Transactions on Acoustics, Speech and Signal Processing*, vol. ASSP-34, no. 10, pp. 1046-1053, Oct., 1986.

APPENDIX

A. Statistical Performance Analysis of D-MNM

The polynomial $D(z)$ is formed with the coefficient vector $\mathbf{d}$ estimated using (14). Any error in the estimated $\mathbf{d}$ would also affect the estimated roots, z_i and the corresponding ω_i's as well the θ_i's. In this Appendix, we analyze the effect on the error in the estimates of the signal zeros z_i due to the error in coefficients estimated by the D-MNM algorithm using (14). The error in the AOAs is also studied. In this summary, the expressions for the first and second moments are given. The complete derivations are omitted for lack of space.

A.1. Effect of Error in the Coefficients on the Mean-Squared Error of the Zeros : The bias in the error of the estimate of z_i is given by,

$$E(\Delta z_i) = \frac{-\sqrt{N}}{\prod_{l=1,l\neq i}^{N-1}(1 - z_l z_i^{-1})}\mathbf{V}'^{H}(e^{j\omega_i})E(\Delta \mathbf{d}') \quad (1)$$

where 'E( )' denotes the expectation operator and $\mathbf{V}'^{T}(e^{j\omega_i}) = \frac{1}{\sqrt{N}}[1, e^{j\omega_i}, \ldots, e^{j(N-2)\omega_i}]$. The mean squared error is given by,

$$E(|\Delta z_i|^2) = \frac{N\mathbf{V}'^{H}(e^{j\omega_i})E(\Delta\mathbf{d}'\Delta\mathbf{d}'^{H})\mathbf{V}(e^{j\omega_i})}{\prod_{l=1,l\neq i}^{N-1}|1 - z_l z_i^{-1}|^2} \quad (2)$$

$$\triangleq \mathbf{S}\ \mathbf{V}'^{H}(e^{j\omega_i})E(\Delta\mathbf{d}'\Delta\mathbf{d}'^{H})\mathbf{V}(e^{j\omega_i}) \quad (3)$$

where, $\mathbf{S} \triangleq \frac{N}{\prod_{l=1,l\neq i}^{N-1}|1-z_l z_i^{-1}|^2}$, denotes the sensitivity of the parameter set [3].

A.2. Coefficient Error due to the D-MNM Method : It can be shown that the error in the coefficients is given by,

$$\Delta\mathbf{d}' = -\mathbf{G}^{\#}\Delta\mathbf{F}_S^H\mathbf{d} \quad (4)$$

where, $\mathbf{G}^{\#} \triangleq \mathbf{G}^H(\mathbf{G}\mathbf{G}^H)^{-1}$ denotes the Moore-Penrose pseudo-inverse of $\mathbf{G}$.

A.3. Bias in the Signal Zeros : It can be shown that the mean of the error in the coefficients is given by,

$$E(\Delta\mathbf{d}') = -\mathbf{G}^{\#}E(\Delta\mathbf{F}_S^H)\mathbf{d} = \mathbf{0}. \quad (5)$$

Substituting (A.5) in (A.1) results in, $E(\Delta\mathbf{z}_i) = \mathbf{0}$. Hence, the bias in the estimate due to the D-MNM method can be expected to be quite small, which was confirmed by simulations.

A.4. Mean Squared Error in the Signal Zeros : Starting with the analysis of $E(\Delta\mathbf{d}'\Delta\mathbf{d}'^{H})$, we can show after rigorous algebraic and statistical manipulation that,

$$E(|\Delta z_i|^2) = \mathbf{S}\mathbf{V}'^{H}(e^{j\omega_i})\mathbf{G}^{\#}\mathbf{D}_S^H\Big(\frac{1}{M}\sum_{g=1}^{N}\sum_{k=1}^{N}d_k d_g^* \ldots$$

$$\Big(\sum_{i=1}^{p}|a_i|^2 e^{j\omega(g-k)} + \sigma_z^2\delta_{gk}\Big)\mathbf{C}\Big)\mathbf{D}_S(\mathbf{G}^H)^{\#}\mathbf{V}'(e^{j\omega_i}) \quad (6)$$

A.5. Mean Squared Error in the AOA Estimates : The expressions for the signal zeros are now related to the errors in the AOA estimates to obtain the final expressions. Since, $z_i = e^{j\omega_i} = e^{j\frac{2\pi d}{\lambda}\sin\theta_i}$ and $z_i^* = e^{-j\frac{2\pi d}{\lambda}\sin\theta_i}$,

$$\frac{dz_i}{d\theta_i} = j\frac{2\pi d}{\lambda}\cos\theta_i e^{j\frac{2\pi d}{\lambda}\sin\theta_i} \approx \frac{\Delta z_i}{\Delta\theta_i} \quad (7)$$

and from this we can write,

$$\Delta z_i = j\frac{2\pi d}{\lambda}\cos\theta_i e^{j\frac{2\pi d}{\lambda}\sin\theta_i}\Delta\theta_i \text{ and} \quad (8)$$

$$\Delta z_i^* = -j\frac{2\pi d}{\lambda}\cos\theta_i e^{-j\frac{2\pi d}{\lambda}\sin\theta_i}\Delta\theta_i. \quad (9)$$

Now we are ready for the final expressions :

$$E(\Delta\theta_i) = \Big(\frac{\lambda}{2\pi d\cos\theta_i}\Big)e^{-j\frac{2\pi d}{\lambda}\sin\theta_i}E(\Delta z_i) = 0 \quad \text{using (9)} \quad (10)$$

$$\text{and also,} \qquad E(|\Delta\theta_i|^2) = \Big(\frac{\lambda}{2\pi d\cos\theta_i}\Big)^2 E(|\Delta z_i|^2). \quad (11)$$

Note that in (A.10), the expression of $E(|\Delta z_i|^2)$ needs to be plugged in from (A.6). It should be emphasized here that unlike the analysis of the classical MNM in [3], our derivation and results do not rely on the statistical properties of the eigenvectors which are neither appropriate nor applicable for the present DFT-based method. Instead the statistics of data are used directly.

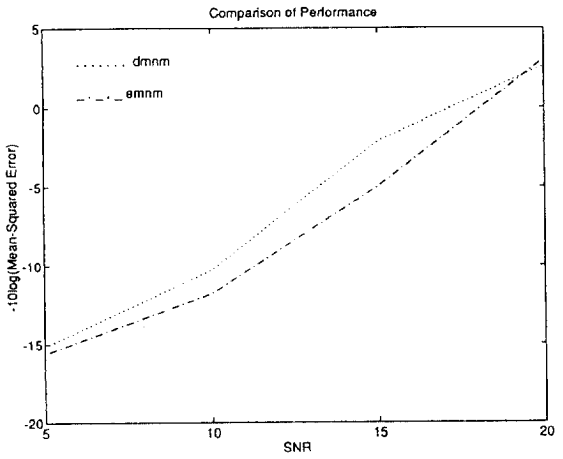

Fig. 1. Comparison of MSEs of D-MNM and E-MNM

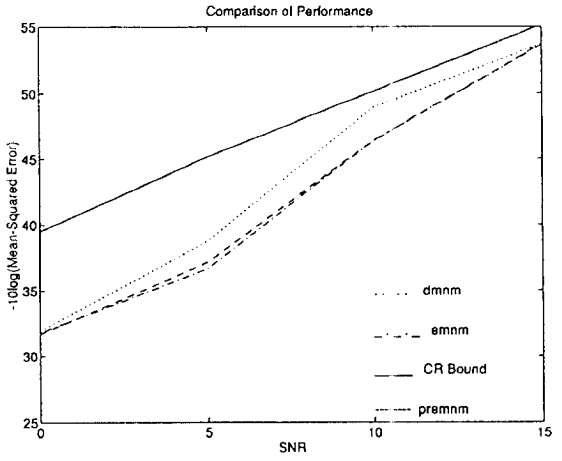

Fig. 4. Comparison of MSEs of D-MNM, TK Meth and CR-bound

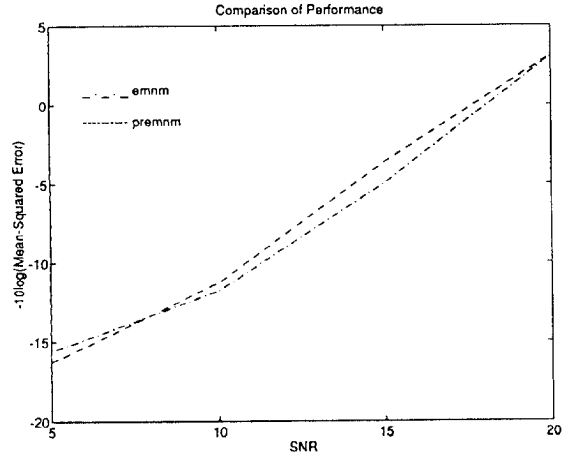

Fig. 2. Comparison of MSEs of P-MNM ($N_S = 4p$) and E-MNM

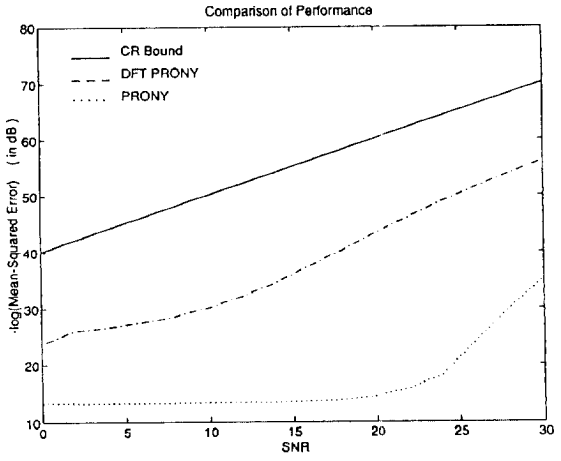

Fig. 5. Comparison of MSEs of Prony and P-Prony

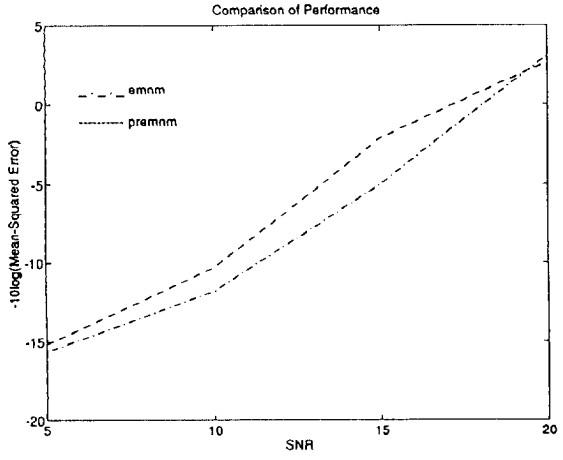

Fig. 3. Comparison of MSEs of P-MNM ($N_S = p$) and E-MNM

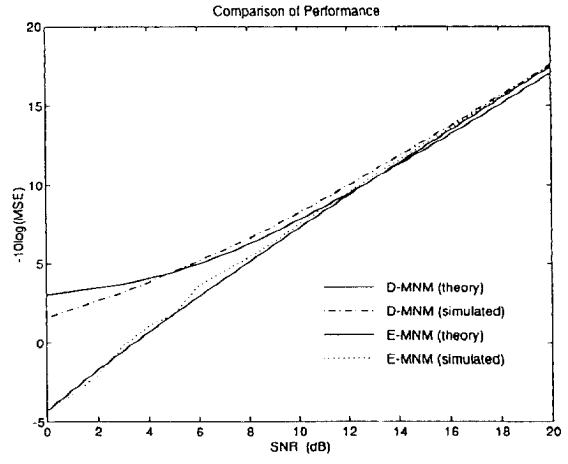

Fig. 6. Comparison of the theoretical and simulated MSEs of D-MNM and E-MNM